Carbohydrate Polymers 98 (2013) 483–489

Contents lists available at SciVerse ScienceDirect

Carbohydrate Polymers

journal homepage: www.elsevier.com/locate/carbpol

Chitin nanofibrils for rapid and efficient removal of metal ions from water system

Dagang Liu*, Yi Zhu, Zehui Li, Donglin Tian, Lei Chen, Peng Chen

Department of Chemistry, Nanjing University of Information Science & Technology, Nanjing, 210044, PR China

ARTICLE INFO

Article history:
Received 26 April 2013
Received in revised form 9 June 2013
Accepted 15 June 2013
Available online 20 June 2013

Keywords:
Chitin
Nanofibril
Heavy metal
Biosorption

ABSTRACT

Joint mechanical defibrillation was successfully used to downsize chitin micro-particles (CMP) into nanofibrils without changing its chemical or crystalline structure. The fine chitin nanofibrils (CNF) bearing width of about 50 nm and length of more than 1 μm were then developed as heavy metal ion sorbents. The uptake performance of CNF dependent on pH, ionic concentration, time, and temperature was investigated. Results show that fixation amount of Cd(II), Ni(II), Cu(II), Zn(II), Pb(II), Cr(III) on CNF was up to 2.94, 2.30, 2.22, 2.06, 1.46, and 0.31 mmol/g, respectively, much higher than CMP due to high specific surface area and widely distributed pores of CNF. Adsorption kinetics of CMP and CNF followed pseudo-second-order model and Freundlich isotherm although CNF exhibited higher rate constant and sorption capacity than that of CMP. The defibrillated CNF is renewable, feasible, easily recyclable, and is thought as good candidate for heavy metal ion treatment due to their low sorption energy, rapid and efficient uptake capacity.

1. Introduction

Toxic heavy metal species mobilized from industrial activities and fossil fuel consumption and eventually are bioaccumulated through the food chain, leading to both ecological and health problems. Recently nanoscopic materials including nanobeads (Türkmen, Yilmaz, Öztürk, Akgöl, & Denizli, 2009), nanocomposites (Liu, Hu, Fang, Zhang, & Zhang, 2009), magnetic nano adsorbents (Huang & Chen, 2009), and nanofibrous matrices (Deng, Bai, & Chen, 2003; Saeed, Haidera, Oh, & Park, 2008), are of great interests developed as efficient adsorbents for metal ions. Among these materials, nanofibrous or nanofibrillar mats have attracted a great deal of attention because of their potential advantages, such as high porosity, high gas permeability, and high specific surface area per unit mass, which might lead to a high fixation ability. Natural polymeric nanofibrils from renewable resources also possess great advantages over micro-sized powder for extracting heavy metals from water or soil; e.g. wool keratose and silk fibroin blend nanofiber mat was thought as a promising candidate as heavy metal ion adsorption filter. The adsorption capacity of Cu(II) was in the range of 14–20 mg/g at pH 8.5 depending on the blend ratio, which was much higher than that of ordinary wool fiber (Baek, Ki, Um, & Park, 2007). Cellulose nanofibers modified with oxolane-2,5-dione exhibited an adsorption of 1.0 and 2.91 mmol/g for Pb and Cd ions from model wastewater samples, respectively (Stephen et al., 2011).

Chitin is a naturally occurring polysaccharide consisting of β (1–4)-2-acetamido-2-deoxy-D-glucose (Jollès & Muzzarelli, 1999; Muzzarelli, 1977; Muzzarelli et al., 2012; Ravi Kumar, Muzzarelli, Muzzarelli, Sashiwa, & Domb, 2004). It is the second most abundant biopolymer after cellulose, existing in the supporting tissues of many organisms. In the organic matrices of mollusk shells or filamentous fungal cell walls, nanofibrillar chitins have the lateral dimensions ranged from 2.5 to 25 nm and self-assembly into the ordered helicoidal phase. However, studies on the natural chitin nanofibrils are limited because of difficulties in isolating and purifying chitin microfibrils or nanofibrils without changing its natural chemical structure, surface charge, or crystalline properties. In recent years, the use of chitin and its derivative materials as biosorbents has gained prominence because of their effective chelation abilities to arsenic, cadmium, cobalt, iron, copper, nickel, manganese, lead, and zinc ions in aqueous system (Shao, Yang, & Shi, 2003). However, as far as we know, nanofibrillar chitin as metal sorbents had never been reported till now.

Several methods have been used to prepare chitin nanofibrils, e.g. preparation of squid pen beta-chitin nanofibrils with 3–4 nm in cross-sectional width and at least a few microns in length were reported by grinding treatment under an acidic condition (pH 3–4) (Fan, Saito, & Isogai, 2008). In our former works, a combined mechanical method, homogenization process and wet-grinding was successfully used to defibrillate chitosan nanofibrils with its natural structure and properties (Liu, Wu, Chang, & Chen, 2011; Liu, Wu, Chang, & Gao, 2011). However, chitosan, an important biosorbents for toxic metal pollutants, is soluble at low pHs and poses problems for developing commercial

* Corresponding author. Tel.: +86 2558731090; fax: +86 2558731090.
E-mail addresses: dagangliu@gmail.com, dagang@gmail.com (D. Liu).

0144-8617/$ – see front matter © 2013 Elsevier Ltd. All rights reserved.
http://dx.doi.org/10.1016/j.carbpol.2013.06.015

Nomenclature

C_e	equilibrium concentration of metal ions (mg L^{-1})
b	Langmuir constant related to the affinity of binding sites (L mg^{-1})
C_0	initial concentrations of metal ions in the aqueous phase (mol L^{-1})
C_i	equilibrium concentrations of metal ions in the aqueous phase (mol L^{-1})
E_a	activation energy (J mol^{-1})
k_1	pseudo-first-order rate constant (min^{-1})
k_2	pseudo-second-order rate constant (g mg^{-1} min^{-1})
k	apparent rate constant
q_e	adsorption amount at equilibrium (mg g^{-1})
q_{max}	maximum capacity (mg g^{-1})
q_t	amount of heavy metal ions adsorbed at any time t (mg g^{-1})
R	gas constant (8.314 J mol^{-1} K^{-1})
T	temperature (K)
V	volume of the solution (L)
W	amount of dry CMP or CNF used (g)

applications. Chitin is difficult to dissolve in organic or inorganic solvents and has a rigid molecular structure and good sorption capacity, therefore, it can provide physical support and increase the accessibility of the metal binding sites for process applications. Herein, we prepared chitin nanofibrils in aqueous system by combined mechanical approaches and investigated the morphology and structure of the obtained chitin nanofibrils. Subsequently, the nanofibrils were developed as an adsorbent for heavy metal ions and the adsorptive behavior of nanofibril was also studied to reveal its potential attractive application in water treatments.

2. Experimental

2.1. Materials

Raw chitin powder with a degree of acetylation of 94% was obtained from Shanghai Jiachen Chemical Company (Shanghai, China), and the other chemicals e.g. nitrate salts of heavy metals and inorganic chemicals of analytical-reagent grade were supplied by Shanghai Chemical Co. (Shanghai, China). The aqueous solutions were prepared by dissolving $Cd(NO_3)_2$, $Cr(NO_3)_3$, $Pb(NO_3)_2$, $Cu(NO_3)_2$, $Ni(NO_3)_2$, and/or $Zn(NO_3)_2$ at different molar ratios in deionized water. The concentration of each metal ion varied from 100 to 5000 ppm.

2.2. Mechanical defibrillation

5 g of raw powder – chitin micro-particles (CMP) was poured into 1 L deionized water and stirred for overnight at room temperature. Then the CMP slurry was poured into wet grinding machine (Labor-pilot 2000/4, IKA® Works, Inc.) with milling gap at about 0.2 mm. The slurry was sheared and passed through the gap with a flow speed of 10 L/h for 10 cycles. And then the obtained chitin slurries were poured into a stainless steel material holding tank of a Microfluidizer (M-100P, Microfluidics Corp.) which was equipped with a diamond interaction chambers (65 μm). Under a constant pressure of 30,000 psi, the slurry passed through the interaction chambers at a rate of 120 mL/min for 10 cycles. The defibrillation process occurred in a special homogenizing valve, in which the fluid passed through a minute gap thereby creating conditions of high turbulence and shear, combined with compression, acceleration, pressure drop, and impact. After wet-grinding or homogenizing process, the homogeneous suspension was obtained by centrifugation at 200 rpm. And the chitin nanofibrils (CNF) were obtained by freeze-drying and then stored in a refrigerator for characterization analysis and sorption tests.

2.3. Characterization

Wide-angle X-ray diffraction (WXRD) studies of the freeze-dried chitin samples were performed with a Siemens D5000 rotating anode wide angle X-ray diffractometer with Cu Kα radiation (λ = 0.154 nm) at 40 kV and 30 mA. X-ray diffraction data were collected from $2\theta = 5–35^\circ$ at a scanning rate of 0.5°/min at room temperature. Scanning electron microscopy (SEM) was performed using an S-570 (Hitachi, Japan) instrument at 20 kV voltage to investigate the surface morphology of the samples. Drop of dilute suspensions of chitin were spread out on the copper grids coated with carbon support film, and then coated with gold prior to observation. Transmission electron microscopy (TEM) observations were carried out on a JEOL JEM 2010 FEF (UHR) electron microscope with an accelerating voltage of 200 kV. Direct examination of CNF structures was carried out by pipetting 2–4 μL of diluted suspension onto a copper grid which had previously been layered with carbon film. Negative staining was carried out applying of about 10 μL of 2% uranyl acetate solution into the grid. In all cases excess liquid was blotted from the sample by lightly touching an edge or corner of filter paper to the edge of the grid. FTIR characterization of CMP or CNF samples in the forms of potassium bromide (KBr) disk were performed with Nicolet Magna 550 FTIR instrument with a frequency range of 4000–400 cm^{-1}. Surface area was measured using Brunauer–Emmett–Teller (BET) nitrogen adsorption method (Micromeritics ASAP 2020). The samples were degassed overnight in a vacuum at 100 °C, and then N_2 gas was used. A relative pressure range, P/P_0, of 0.05–0.3 was used for calculating the BET surface area.

2.4. Batch adsorption studies

The adsorption of heavy metals on CMP and CNF was carried out using the batch method. In sorption experiments, a fixed amount of dry CMP or CNF (0.1 g) suspended in deionized water (100 g) was poured into a glass-stoppered flask, and then solution containing heavy metal ions like Cd(II), Pb(II), Ni(II), Cu(II), and Cr(III) were added into above-prepared suspension of CMP or CNF and shaken at 10 rpm for 72 h using a thermostated shaker at 25 °C. After equilibrium the suspensions were centrifuged for 2 min at 12,000 rpm to remove CMP or CNF with adsorbed heavy metal ions. The concentrations of metal ions remained in the supernatant were measured using the atomic absorption spectrophotometer (AAS, Model 3510, Agilent Tech). Each test was three-times duplicated at least under identical conditions. The amount of metal ions adsorbed q (mol/kg) was obtained by the following equation:

$$q = \frac{(C_0 - C_i)V}{W} \quad (1)$$

where C_0 and C_i are the initial and equilibrium concentrations of metal ions in the aqueous phase (mol/L) respectively; V is the volume of the solution (L) and W is the amount of dry CMP or CNF used (g). During the adsorption process, dependence of the initial concentration, contact time, temperature, pH on the adsorption behavior was investigated thoroughly. The corresponding supernatants were immediately centrifuged, collected, and diluted for concentration analysis by AAS.

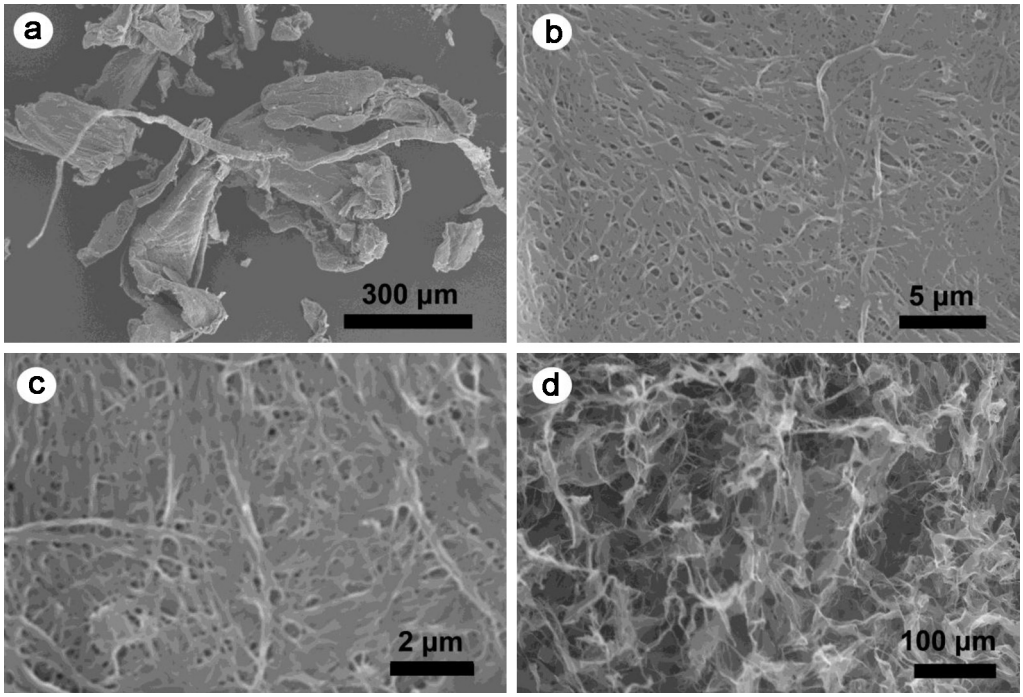

Fig. 1. SEM micrographs of raw chitin particles (a), wet-ground microfibrils (b and c), freeze-dried CNFs after homogenization (d), respectively.

3. Results and discussion

3.1. Morphology and structure of CMP and CNF

SEM micrographs of raw chitin particles (a), wet-ground microfibrils (b and c), and freeze-dried nanofibrils after high pressure homogenization (d) are shown in Fig. 1. The raw chitin particles as shown in Fig. 1a have irregular forms and average size over 10 μm, and some CMP fibers were also observed to have a millimeter scale level. In nature, fibrous chitin is the main component of some biological organs, such as cell walls of fungi, the exoskeletons of arthropods or crustaceans and insects, the radulas of mollusks, and the beaks of squid and octopuses Ravi Kumar, Muzzarelli, Muzzarelli, Sashiwa, & Domb, 2004. After strong mechanical grinding for 5 cycles, the fibrous particles were split away and broken into finer fibers (Fig. 1b). Subjected to continuous mechanical shear force, the fibers were downsized to form network of microfibrils (Fig. 1c). After continuing treatment by high pressure homogenization, the defibrillated nanofibril was linked to form into branch-shaped network with porous structure (Fig. 1d). To describe the detailed morphology of the CNF, Fig. 2 exhibits the unstained CNF (a and b), and negative stained CNF (c and d). The nanofibrils were crosslinked and generated a porous network form, in which the fibrils had a width of about 50 nm and length over 1 μm. X-ray diffraction pattern of the nanofibrils in the selected area (inner of Fig. 2a) produced bright rings that are characteristic of semi-crystalline chitin. After removing the large microfibrillar particles by slightly centrifugation, isolated nanofibrils displayed an aspect ratio over 50. In Fig. 2d, nanofibrils supported by carbon film were observed to possess sub-leveled fibrils with diameter ranged from 1 to 30 nm, which are similar to our former work on chitosan nanofibrils by mechanical treatments (Liu, Wu, Chang, & Chen, 2011). It is a highly efficient downsizing process to defibrillate or disassemble chitin macro-hierarchy, to associated microfibril bundles, and to nanofibrils step by step. It is worth noting that the obtained CNF had a specific area of 68.43 m^2/g, much higher than that of CMP (2.16 m^2/g). Therefore, nanofibrillar chitin with higher specific area and pore distribution provided encouraging inspiration for artificial biosorbents.

FTIR spectra of CMP and CNF is shown in Fig. 1S (supplementary information). Both CMP and CNF show resonance bands at 1154 and 893 cm^{-1} attributed to saccharide groups. The OH stretching band at 3482 cm^{-1}, NH stretching band at 3270 cm^{-1}, amide band I at 1661 and 1622 cm^{-1}, and amide II band at 1559 cm^{-1} of CMP and CNF are also identified their chitin structure. Meanwhile, the relative intensity of amide in CNF did not decrease, which means that chitin was not derived into chitosan by deacetylation. Fig. 2S (supplementary information) shows the X-ray diffraction profiles of CMP and CNF. As a semicrystalline polymer, four diffraction peaks of the chitin nanofibrils at $2\theta = 9.2$, 19.1, 20.9, 23.1 and 26.4° corresponded to 0 2 0, 1 1 0, 1 2 0, 1 3 0 and 0 1 3 planes, respectively (Zhang, Xue, Xue, Gao, & Zhang, 2005), and these diffraction patterns of both CMP and CNF coincide closely, exhibiting typical antiparallel crystal patterns of α-chitin. The relative crystalline index of CNF determined from X-ray diffraction profiles is 68%, which is almost equal to CMP (66%). Therefore, the original chemical and crystalline structure was retained after the strong joint mechanical treatment.

3.2. Effects of pH on sorption capacity

Effects of pH on ionic adsorption by CNF were investigated and the results are presented in Fig. 3. The sorption capacity of Ni(II), Zn(II), Cd(II), Pb(II) and Cu(II) ions increased with the increase of pH from 1 to 5 except the case of Cr(III). In acid condition, the chelation sites of chitin were occupied by hydrion of added acid; when metal ions entered the system, a competitive reaction drove hydrion away from those sites, which means that less proton would benefit for higher fixation of metal ions. That is why Ni(II), Zn(II), Cd(II), Pb(II) ions showed a double and even 40-folds heavier loading on CNF at pH 5 than that at pH 1. Therefore, sorption and desorption of these metal ions could be well controlled by adjusting pH of the suspension. However, adsorption capacity of Cu(II) or Cr(III) ions

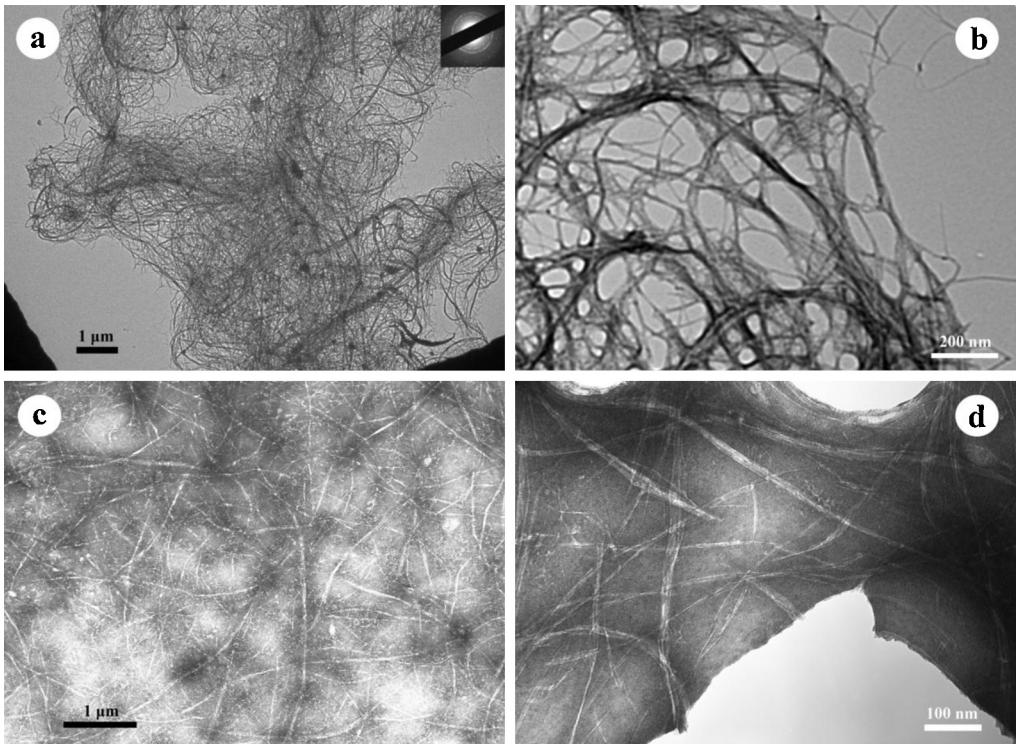

Fig. 2. TEM micrographs of unstained chitin microfibrils (a and b), and negative stained CNFs (c and d).

did not change too much with varying pH, perhaps contributed to their competitive binding ability or hydrolysis at higher pH value.

3.3. Maximum sorption capacity

Adsorption capacity as a function of initial concentration of Cd(II), Pb(II), and Ni(II) ions is shown in Fig. 3S (supplementary information). The adsorption capacity of CNF exhibited a highly concentration dependent phenomenon. At low concentration, the adsorption capacity sharply increased with the increment of ionic concentration because the active sites of CNF were enough to combine ions. Furthermore, with the increase of concentration, ionic adsorption on CNF gradually arrived to saturated balance, which was noted as a maximum value (q_{max}). When the concentration was higher than saturation, overmuch ions would fail to occupy the same adsorption sites and had to go through without being adsorbed. The values of q_{max} for six heavy metal ions adsorbed on CNF are analyzed and summarized in Table 1. CNF exhibited a great affinity to heavy metal ions, and its q_{max} for Cd(II), Ni(II), Cu(II), Zn(II), Pb(II), and Cr(III) were 2.94, 2.30, 2.22, 2.06, 1.46 and 0.31 mmol/g, respectively. It is well known that complex could be formed between heavy metal ions and chitin or chitosan due to their strong chelation action of miscellaneous functional groups such as hydroxyl, carbonyl, and amide (or amine) groups. In general, chitosan biopolymer demonstrated greater fixation ability for heavy metal ions than chitin; therefore, chitin is not so applicable in heavy metal sorption as chitosan because it is difficult to be dissolved or dispersed in water or other solvents but chitosan can be dissolved in acid solvents. E.g. only few reports about chitin adsorbent is that its q_{max} for Cd(II) was 93.9 mg/g (Xiong, 2010), whereas chitosan was reported to chelate five to six times greater amounts of metals than chitin, attributed to the free amine groups bearing on chitosan (Yang & Zall, 1984), e.g. the saturated adsorption capacities of chitosan was 0.3, 1.5–2.5, 0.6–1.3, 2.0, 0.2 and 0.94 mmol/g corresponding to Cr(III), Cu(II), Cd(II), Ni(II), Pb(II), and Zn(II), respectively (Eric, 2004). However, CNF in this work exhibited higher adsorption capacities than those reported chitin or chitosan sorbents. This perhaps provided a new evidence that metal ionic chelation ability of chitin was not lower than that of chitosan.

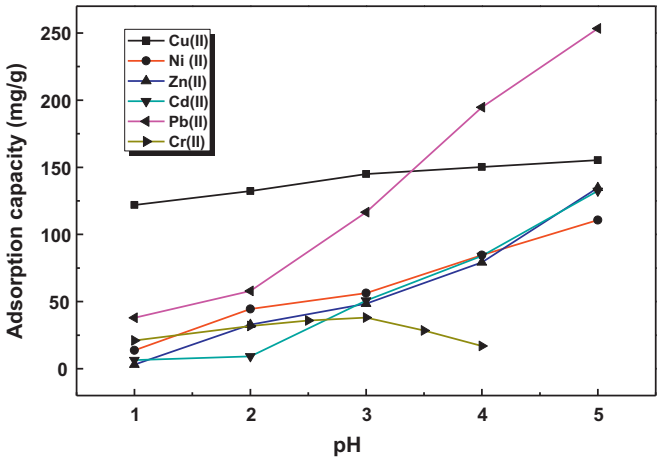

Fig. 3. Effects of pH on the adsorption capacity of metal ions by CNF.

Table 1
Adsorption capacities of various heavy metal ions for CMP and CNF.

Metal ions	q_{max} of CMP		q_{max} of CNF	
	mg/g	mmol/g	mg/g	mmol/g
Cd(II)	59.42	0.53	330.15	2.94
Ni(II)	42.62	0.73	134.72	2.30
Cu(II)	23.45	0.37	141.08	2.22
Zn(II)	38.36	0.59	134.03	2.06
Pb(II)	198.19	0.96	303.49	1.46
Cr(III)	6.40	0.12	16.28	0.31

Table 2
Langmuir and Freundlich isotherm parameters for metal ions binding to CNF.

Metal ions	Measured	Langmuir			Freundlich		
	q_{max} (mg/g)	Q_{max} (mg/g)	b (L/mg)	R^2	$1/n$	K_F (mg/g)	R^2
Pb(II)	303.9446	−909.0910	−0.2484	0.2450	1.2543	0.0536	0.9160
Ni(II)	177.1100	344.8276	0.0019	0.6027	0.7510	1.7418	0.8853
Cd(II)	254.9500	−3333.3330	−0.1505	0.0678	1.0666	0.3574	0.9643

Simultaneously, sorption capacity by CMP is also investigated and listed in Table 1. q_{max} value by CMP is 5–6 times lower than that of CNF, especially in the case of Cd(II) and Cu(II) ions, indicating that large specific surface area, highly distributed pores, and high aspect ratio of the CNF played key roles in adsorption capacity of CNF. It is interesting that the q_{max} value for six metal ions by CMP or CNF had a different order, which was perhaps contributed to the fact that those heavy metal ions with varied ionic radius and charge exhibited different ability of penetration or adhesion onto CMP or CNF sorbents.

3.4. Sorption isotherm

Langmuir and Freundlich models are two major isotherms for fitting the experimental data and describe the distribution of the adsorbate species among solid and liquid phases (Freundlich, 1906; Langmuir, 1916). The Langmuir adsorption isotherm can be expressed as:

$$\frac{C_e}{q_e} = \frac{1}{q_{max}} C_e + \frac{1}{q_{max} b} \quad (2)$$

where C_e is the equilibrium concentration of metal ions (mg/L), q_e is the adsorption amount at equilibrium (mg/g), q_{max} is the maximum capacity (mg/g), and b is the Langmuir constant related to the affinity of binding sites (L/mg). The Langmuir model assumes that uptake of metal ion occurs on a homogenous surface by monolayer sorption without any interaction between adsorbed ions. And the linear form of the Freundlich isotherm is expressed as:

$$\lg q_e = \log K_F + \frac{1}{n} \log C_e \quad (3)$$

where K_F is roughly an indicator of the adsorption capacity, $1/n$ is of the adsorption intensity. The magnitude of the exponent $1/n$ gives an indication of the favorability of adsorption. The value of n is more than 1, which represent favorable adsorption condition. The Freundlich equation is an empirical model to describe the adsorption on a heterogeneous surface.

Based on tested data, the parameters from Langmuir and Freundlich model are calculated and listed in Table 2. The fitness of the data was evaluated using coefficient of determination (R^2). Based on the coefficient of determination values for the two models, the Freundlich model fitted the isotherm equilibrium data reasonably well with R^2 values closer to 1, that is, the equilibrium data were more satisfactorily fitted to the Freundlich isotherm than the Langmuir isotherm model. On average, a favorable adsorption tends to have Freundlich constant n between 1 and 10 (Delle, 2001). Higher value of n (smaller value of $1/n$) implies stronger interaction between CNF and heavy metal while $1/n$ equal to 1 indicates linear adsorption leading to identical adsorption energies for all sites, e.g. in the case of Cd(II) ion.

3.5. Sorption kinetics

Adsorption reaction was always greatly dependent on contact time. Fig. 4 shows effects of contact time on the adsorption capacity of Cd(II), Pb(II), and Ni(II) ions by CMP and CNF. At the initial few minutes (0–5 min), CNF exhibited a fast and efficient uptake of heavy metal ions, e.g. the uptake of Cd(II) ion after 3 min increased from 0 to 157 mg/g, which means that CNF had taken 97% ions from its equilibrium capacity. One hour later, adsorptive reactions basically achieved equilibrium. In the case of Pb(II) and Ni(II) ions, the adsorption amount at 5 min was 243.65 mg/g and 78.95 mg/g, accounting for 83% and 59% of their equilibrium adsorption capacity, respectively. Although CMP exhibited the similar sorption profile with extended time, much lower ionic uptake and longer equilibrium sorption time can be obviously observed from Fig. 4. The slope of initial sorption curve of CMP is lower than that of CNF indicating a higher ionic sorption rate for nanosized chitin fibers. Therefore, it can be concluded that adsorption of Cd(II),

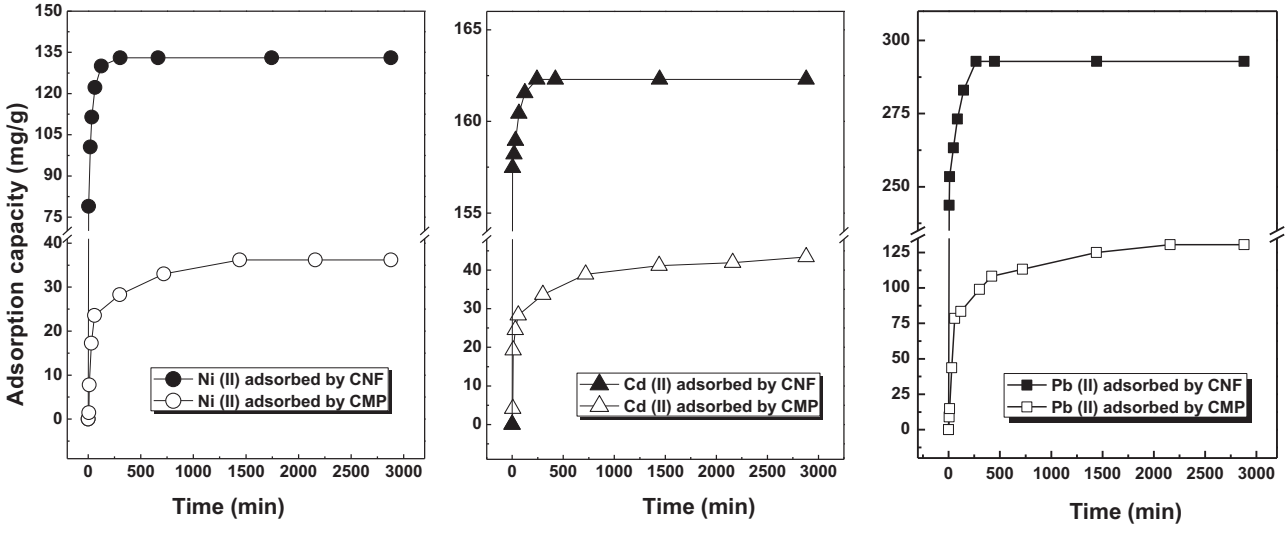

Fig. 4. Effects of contact time on the adsorption capacity of Ni(II), Cd(II), Pb(II) by CNF and CMP.

Table 3
Kinetic parameters of regression equations for heavy metal ions sorption onto CNF and CMP.

Adsorbents	Metal ions	Measured	Pseudo-first-order			Pseudo-second-order		
		q_e	R^2	k_1	Calculated q_e	R^2	k_1	Calculated q_e
CNF	Cd(II)	162.29	0.9972	0.01589	5.34	0.9999	0.0167	162.69
	Pb(II)	292.86	0.8354	0.01612	77.82	0.9991	0.0024	292.86
	Ni(II)	133.03	0.9684	0.03524	82.38	0.9999	0.0003	133.03
CMP	Cd(II)	43.417	0.8879	0.0014	20.012	0.9994	0.0004	43.668
	Pb(II)	130.545	0.8903	0.0021	77.268	0.9996	0.0001	133.334
	Ni(II)	36.179	0.8786	0.0030	23.329	0.9995	0.0004	36.901

Table 4
Activation energy calculated from the pseudo-second-order kinetic model for Pb(II), Ni(II) and Cd(II) ions adsorbed by CNF.

Metal ions	Temperature (K)	q_e (mg/g)	Apparent rate constant k	E_a (J/mol)
Pb(II)	298.15	292.86	0.0024	–
	343.15	116.51	0.0002	0.00002
Ni(II)	298.15	133.03	0.0003	–
	343.15	93.89	0.0002	0.00013
Cd(II)	298.15	162.29	0.0167	–
	343.15	113.10	0.0035	0.00003

Pb(II) and Ni(II) on CNF could be achieved momentarily with high efficiency and capacity.

Predicting the rate of adsorption for a given system is the most important factors in adsorption system design, because the system's kinetics was determined by adsorbate time and the reactor dimensions (Ho, 2006). Of all heavy metal adsorption kinetic models, model for pseudo-first-order kinetics and pseudo-second-order kinetics are most widely used. The expression of pseudo-first-order kinetic model is expressed as follows:

$$\frac{dq_t}{dt} = k_1(q_e - q_t) \tag{4}$$

Linear form of this model obtained by integral can be expressed as Eq. (5).

$$\lg(q_e - q_t) = \lg\ q_e - \frac{k_1 t}{2.303} \tag{5}$$

where k_1 is the pseudo-first-order rate constant (min^{-1}), q_e and q_t are the amount of heavy metal ions adsorbed at equilibrium ($mg\,g^{-1}$) and at time t ($mg\,g^{-1}$), respectively. Such an equation should yield a straight line with intercept equal to $\lg q_e$ and slope equal to $-(k_1/2.303)$. As seen from the Eq. (5), the pseudo-first-order kinetic model is based on the assumption that adsorption was controlled by diffusion steps, and the rate of adsorption is in direct proportion to the difference value of equilibrium adsorption capacity and the adsorption capacity at time t.

While the expression of pseudo-second-order kinetic model is given by following:

$$\frac{dq_t}{dt} = k_2(q_e - q_t)^2 \tag{6}$$

Linear form of this model obtained by integral can be expressed as Eq. (7).

$$\frac{t}{q_t} = \frac{1}{k_2 q_t^2} + \frac{t}{q_e} \tag{7}$$

where k_2 is the pseudo-second-order rate constant ($g\,mg^{-1}\,min^{-1}$), q_e and q_t are the amount of heavy metal ions adsorbed at equilibrium ($mg\,g^{-1}$) and at time t ($mg\,g^{-1}$), respectively. Also it could yield a straight line with intercept equal to $1/k_2 q_t{}^2$ and slope equal to $1/q_e$.

Based on the experimental results from Fig. 4, pseudo-first-order and the pseudo-second-order dynamic models were established and are shown in Fig. 4S (supplementary information), respectively. The curves were fit and the parameters of regression equations corresponding to the curves from the pseudo-first-order and pseudo-second-order dynamic model were calculated and listed in Table 3. It is found that the linear correlation coefficients (R^2) from the pseudo-second-order model were closer to 1 than those from the pseudo-first-order dynamic model, and furthermore the calculated q_e of Cd(II), Pb(II), and Ni(II) from pseudo-second-order dynamic model was almost equal to the measured value of q_e. Therefore, the adsorption of metal ions on CNF was in line with the pseudo-second-order kinetic model. To compare with CNF, we also calculated the kinetic model and regression parameters of CMP and listed them in Table 3. The pseudo-second-order kinetic model was also fitted for sorption behavior of CMP, which means either CMP or CNF had the same adsorption mechanism to metal ions. Normally, the mechanism of rate control about pseudo-second-order model was thought as chemical adsorption.

3.6. Sorption active energy

Fig. 5S (supplementary information) depicts effects of temperature on the adsorption capacity of metal ions by CNF. The sorption capacity of Ni(II), Zn(II), Cd(II), Cr(III), Cu(II) ions slightly decreased with increasing temperature from 30 to 70 °C, in the case of Pb(II), the sorption capacity decreased sharply from 292 at 30 °C to 116 at 70 °C, indicating that the adsorption process is exothermic. It was thought that the sorption capacity reduced since CNF tended to aggregate with increasing temperature. According to Arrhenius equation, activation energy of the adsorption (E_a; J/mol) can be calculated using the following equation:

$$\ln\frac{k(T_2)}{k(T_1)} = \frac{E_a}{R}\left(\frac{1}{T_1} - \frac{1}{T_2}\right) \tag{8}$$

where k is the apparent rate constant; E_a is the activation energy; R is the gas constant (8.314 J/mol K); T is the temperature (K). According to the parameters of pseudo-second-order kinetic model, sorption activation energies of Pb (II), Ni (II), and Cd(II) are calculated and summarized in Table 4. As seen from the table, the value of E_a related to these metal ions was nearly zero, indicating that the energetic barrier against the adsorption of metal ion was easier to overcome, therefore, adsorption process was feasible and spontaneous.

4. Conclusions

This study provided an efficient way of preparing chitin nanofibrils and adsorbing heavy metal ions in aqueous system by CNF. CNF exhibited similar sorption behavior to CMP, such as, Freundlich isotherm, pseudo-second-order kinetics, and concentration or pH dependence. However, counting on the high specific surface area, widely distributed pores, and more accessible chelating groups, CNF had a high adsorption capacity of Cd(II), Cu(II), Pb(II), and Ni(II) up to 330.15 mg/g, 141.08 mg/g, 303.49 mg/g, and 134.72 mg/g, respectively, which was much higher than CMP, and even higher than those reported chitosan sorbents. And what is more, adsorption capacity of metal ions by CNF could achieve 80% of their saturated adsorption amount only in 10 min, indicating a rapid, spontaneous, and efficient sorption process.

Acknowledgements

The authors are grateful to National Natural Science Foundation of China (Nos. 51103073 and 21277073), Natural Science Foundation of Jiangsu Province (No. BK2011828) and Qing Lan Project of Jiangsu Province for financial support.

Appendix A. Supplementary data

Supplementary data associated with this article can be found, in the online version, at http://dx.doi.org/10.1016/j.carbpol.2013.06.015.

References

Baek, D. H., Ki, C. S., Um, I. C., & Park, Y. H. (2007). Metal ion adsorbability of electrospun wool keratose/silk fibroin blend nanofiber mats. *Fibers and Polymers*, *8*, 271–277.

Delle, Site A. (2001). Factors affecting sorption of organic compounds in natural sorbent/water systems and sorption coefficients for selected pollutants. A review. *Journal of Physical and Chemical Reference Data*, *30*, 187–439.

Deng, S., Bai, R., & Chen, J. P. (2003). Aminated PAN fibers for lead and copper removal. *Langmuir*, *19*, 5058–5064.

Eric, G. (2004). Interactions of metal ions with chitosan-based sorbents: A review. *Separation Science and Technology*, *38*, 43–74.

Fan, Y., Saito, T., & Isogai, A. (2008). Preparation of chitin nanofibers from squid pen beta-chitin by simple mechanical treatment under acid conditions. *Biomacromolecules*, *9*, 1919–1923.

Freundlich, H. M. F. (1906). Über die adsorption in läsungen. *Zeitschrift für Physikalische Chemie*, *57*, 385–470.

Ho, Y. S. (2006). Review of second-order models for adsorption systems. *Journal of Hazardous Materials*, *136*, 681–689.

Huang, S., & Chen, D. (2009). Rapid removal of heavy metal cations and anions from aqueous solutions by an amino-functionalized magnetic nano-adsorbent. *Journal of Hazardous Materials*, *163*, 174–179.

Jollès, P., & Muzzarelli, R. A. A. (Eds.). (1999). *Chitin and chitinases*. Basel: Birkhauser Verlag.

Langmuir, I. (1916). The constitution and fundamental properties of solids and liquids. *Journal of the American Chemical Society*, *38*, 2221–2295.

Liu, D., Wu, Q., Chang, P. R., & Chen, M. (2011). Chitosan colloidal suspension composed of mechanically-disassembled nanofibers. *Journal of Colloid and Interface Science*, *354*, 637–643.

Liu, D., Wu, Q., Chang, P. R., & Gao, G. (2011). Self-assembled liquid crystal film from mechanically-defibrillated chitosan nanofibers. *Carbohydrate Polymers*, *84*, 686–689.

Liu, X., Hu, Q., Fang, Z., Zhang, X., & Zhang, B. (2009). Magnetic chitosan nanocomposites: A useful recyclable tool for heavy metal ion removal. *Langmuir*, *25*, 3–8.

Muzzarelli, R. A. A. (1977). *Chitin*. Oxford: Pergamon Press.

Muzzarelli, R. A. A., Boudrant, J., Meyer, D., Manno, N., DeMarchis, M., & Paoletti, M. G. (2012). A tribute to Henri Braconnot, precursor of the carbohydrate polymers science, on the chitin bicentennial. *Carbohydrate Polymers*, *87*, 995–1012.

Ravi Kumar, M. N. V., Muzzarelli, R. A. A., Muzzarelli, C., Sashiwa, H., & Domb, A. J. (2004). Chitosan chemistry and pharmaceutical perspectives. *Chemical Reviews*, *104*, 6017–6084.

Saeed, K., Haidera, S., Oh, T. J., & Park, S. Y. (2008). Preparation of amidoxime-modified polyacrylonitrile (PAN-oxime) nanofibers and their applications to metal ions adsorption. *Journal of Membrane Science*, *322*, 400–405.

Shao, J., Yang, Y., & Shi, C. (2003). Preparation and adsorption properties for metal ions of chitin modified by L-cysteine. *Journal of Applied Polymer Science*, *88*, 2575–2579.

Stephen, M., Catherine, N., Brenda, M., Andrew, K., Leslie, P., & Corrine, G. (2011). Oxolane-2,5-dione modified electrospun cellulose nanofibers for heavy metals adsorption. *Journal of Hazardous Materials*, *192*, 922–927.

Türkmen, D., Yilmaz, E., Öztürk, N., Akgöl, V., & Denizli, A. (2009). Poly(hydroxyethyl methacrylate) nanobeads containing imidazole groups for removal of Cu(II) ions. *Material Science and Engineering: C*, *29*, 2072–2078.

Xiong, C. (2010). Adsorption of cadmium (II) by chitin. *Journal of the Chemical Society of Pakistan*, *32*, 429–435.

Yang, T. C., & Zall, R. R. (1984). Adsorption of metals by natural polymers generated from sea food processing wastes. *Industrial and Engineering Chemistry Product Research and Development*, *23*, 168–172.

Zhang, Y., Xue, C., Xue, Y., Gao, R., & Zhang, X. (2005). Determination of the degree of deacetylation of chitin and chitosan by X-ray powder diffraction. *Carbohydrate Research*, *340*, 1914–1917.